

Continuously Voltage-Tunable Line Absorption in Surface Quantization*

R. G. Wheeler and R. W. Ralston

Mason Laboratory, Yale University, New Haven, Connecticut 06520

(Received 16 August 1971)

Photoconductance response due to optical transitions induced by 44.3-meV laser radiation between surface subbands in the inversion layer on a (001) surface of *p*-type silicon is reported. The negative response indicates decreased mobility of electrons in the excited states. Magnetic fields normal to the surface accentuate the response for certain levels because of parallel-motion band mixing. These measurements are the first to demonstrate the large voltage tunability inherent in this electronic energy level system.

Oscillatory magnetoconductance measurements of narrow inversion channels on (001) silicon surfaces have demonstrated the existence of quantized levels in the electron motion normal to the surface.^{1,2} Duke has calculated for a realistic model the optical absorption coefficients for electric dipole transitions between the occupied ground state and higher unoccupied excited states.³ The energy level spacing is a strong function of the potential defining the channel, hence any absorption may be modulated by a voltage applied between a field plate (gate) and the conduction channel. We report on the observation of channel conductance modulation in a metal-oxide-semiconductor (MOS) silicon device induced by voltage resonant tuning to energy level differences of 44.3 meV (27.97 μm) when irradiated with a H_2O molecular laser.

An *n*-type inverted channel is produced at the (001) surface of *p*-type silicon when the energy bands are bent by the action of a gate voltage such that the bottom of the conduction band is near the Fermi level. For this case Howard and Stern have shown, neglecting immobile surface charges, that the potential for mobile electrons near the surface will be triangular with a field normal to the surface given by $F = (2E_g N_A / \epsilon)^{1/2}$ just at that gate voltage V_T at which mobile charges begin to occupy the channel.⁴ In mks units, E_g is the band gap, N_A the bulk acceptor concentration, and ϵ the dielectric constant of silicon. Assuming the effective-mass approximation for this well, the energy levels are given by

$$E = E_{ci} + \frac{\hbar^2}{2m_x^2} K_x^2 + \frac{\hbar^2}{2m_y^2} K_y^2, \quad (1)$$

where E_{ci} is the solution of the Schrödinger equation with a linear potential eFz for $z > 0$:

$$E_{ci} = -[(ehF)^{2/3} / (2m_z)^{1/3}] S_i. \quad (2)$$

Here S_i is the *i*th solution of $\text{Ai}(s) = 0$, with $\text{Ai}(s)$ the Airy function.^{5,6} Because of the nature of the

band structure of silicon, described by six mass ellipsoids oriented along $\langle 001 \rangle$ and equivalent directions, m_z will have two values $0.98m_e$ and $0.19m_e$ for a (001) surface. This gives rise to two energy level ladders neglecting valley-degeneracy splitting. Associated with each mass ladder there will be distinct and different two-dimensional bands describing the motion parallel to the surface where k_x and k_y are measured relative to the conduction-band minima. For the heavy-mass ladder an isotropic conduction mass exists with $m = 0.19m_e$, and for the light-mass ladder $m_x = 0.19m_e$, $m_y = 0.98m_e$ are derived from the $\langle 100 \rangle$ ellipsoids. Electric dipole transitions can be induced between these electric subbands with the photon electric field vector perpendicular to the interface. If only the ground state is occupied, two types of transitions may occur, those to subbands having a curvature identical to the ground state, ideally characterized by a sharp line absorption, and those to subbands having a different curvature, hence a broad and weaker absorption.

Inversion necessitates a self-consistent solution of Poisson's and Schrödinger's equations to determine the spatial extent of the mobile charge distribution, hence the potential and energy levels. The calculations of Stern and Howard for $N_A = 10^{15}/\text{cm}^3$ and for mobile charge density $n_s \leq 5 \times 10^{12}$ electrons/ cm^2 show that the potential is significantly modified only for the ground state. One can then visualize the triangular well nearly unaffected for the excited states with the gate voltage depressing only the ground state. Thus the separation between excited states is set by the bulk doping level and the ground state is tuned with increasing inversion. The potential diagram of Fig. 1 has been constructed for the case at hand.

A MOS *p*-type silicon two-terminal capacitor was fabricated using standard techniques.⁷ The geometry of the field plate was an ellipse 1×2.5

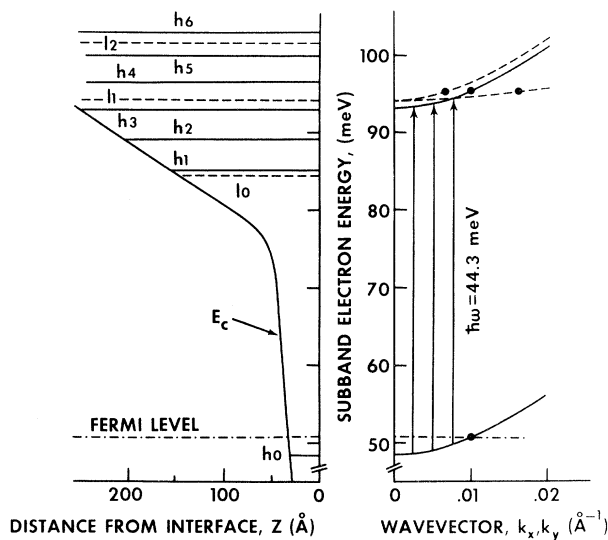


FIG. 1. The quantizing potential with associated normal-motion binding energies is indicated for a composite triangular well model. The known acceptor density $N_A = 2 \times 10^{14}/\text{cm}^3$ determines the depletion field of 8.4×10^3 V/cm. A surface field of 1.5×10^5 V/cm is shown for an electron sheet of $10^{12}/\text{cm}^2$ which consists of both mobile subband charge and immobile interface charge. The fitting of the two triangles into a model well is done schematically to force the h_0 - h_3 energy splitting to be 44.3 meV which is the photon energy of the incident laser radiation. Associated dispersion curves for the h_0 , h_3 , and l_1 parallel-motion subbands are also indicated, the nonresonant subbands being omitted for clarity. Dots on the dispersion plot indicate the first Landau state for the subbands with an imposed magnetic field $B_z = 70$ kG.

mm with a 1500-\AA SiO_2 dielectric forming the gate structure. Starting with $40\text{-}\Omega\text{-cm}$ p -type material, device interfacial states were determined to be about $8 \times 10^{11}/\text{cm}^2$ by the temperature dependence of the threshold voltage necessary for inversion.⁸ The equivalent circuit of the structure at 4.2°K is the dielectric capacitance of 500 pF in series with the channel resistance of about 100 k Ω caused by a $25\text{-}\mu\text{m}$ gap between the edge of the field plate and the n^+ diffused electron source. The silicon chip was beveled at the narrow edges on the back side at a 45° angle so that the radiation from a H_2O molecular laser could pass to the channel and then be reflected out of the device to a photodetector. Provision was made to apply a magnetic field of 70 kG perpendicular to the surface.

Direct absorption measurements were attempted unsuccessfully. With only a single pass to the surface, the expected absorption for a 2-meV linewidth ranged between 10^{-4} to 10^{-5} , a require-

ment on the laser stability we were unable to achieve. Thus the conductance measurement was undertaken, letting the device act as its own detector. We can represent the channel conductance as $G = n_1 e \mu_1 + n_2 e \mu_2$, where n_1 is the number of electrons in the ground subband, n_2 the number in the excited subband, and $\mu_{1,2}$ the carrier mobilities in the respective bands. Here

$$n_1 + n_2 = n_s \epsilon_{\text{ox}} (V_g - V_T) / ed, \quad (3)$$

a constraint imposed by the gate voltage V_g relative to the threshold voltage V_T , where ϵ_{ox} is the oxide dielectric constant and d the oxide thickness. Clearly $n_2 = \dot{n} \alpha \tau$, where \dot{n} is the resonant photon flux, α the absorption which is a functional of n_s , and τ the excited-state lifetime. Thus we search for channel conductivity modulation, assuming $\mu_1 \neq \mu_2$, which occurs when the gate voltage resonates the subband level differences with the photon energy 44.3 meV. Since the device is a two-terminal one, the change in channel resistance was detected by double-sideband amplitude-modulation techniques. A small 5000-Hz voltage signal was superimposed on the slow gate-voltage sweep. The laser radiation was mechanically chopped at 500 Hz, and thus the conductivity modulation is detected at 500 Hz following suitable amplifiers, filters, and demodulators. Especial care was taken in the phasing of the detected signal relative to the light phase on the device. We recorded both conductance changes, in phase and out of phase with the light.

At real Si-SiO_2 interfaces fabricated by techniques similar to ours, Gray and Brown determined the distribution of interface states in the forbidden gap near the conduction and valence bands.⁹ Their results for inversion imply a broad distribution of negatively charged states (acceptors) peaked about 100 meV below the band. With weak inversion these acceptors are photoionized to the lowest subband. As inversion is increased, the Fermi level moves to higher energy relative to the interfacial distribution. Thus this photoresponse turns on below the threshold for dark channel conductance, attains a maximum at an intermediate value of channel current, and then decreases to zero when the Fermi level is more than 44.3 meV above the tail of the distribution. The recombination rate may be characterized as "slow,"¹⁰ since the magnitude of the photoconductivity out of phase with the chopped laser beam is nearly the same as the in-phase component. This process of conductivity increase will compete with a conductivity change due to absorp-

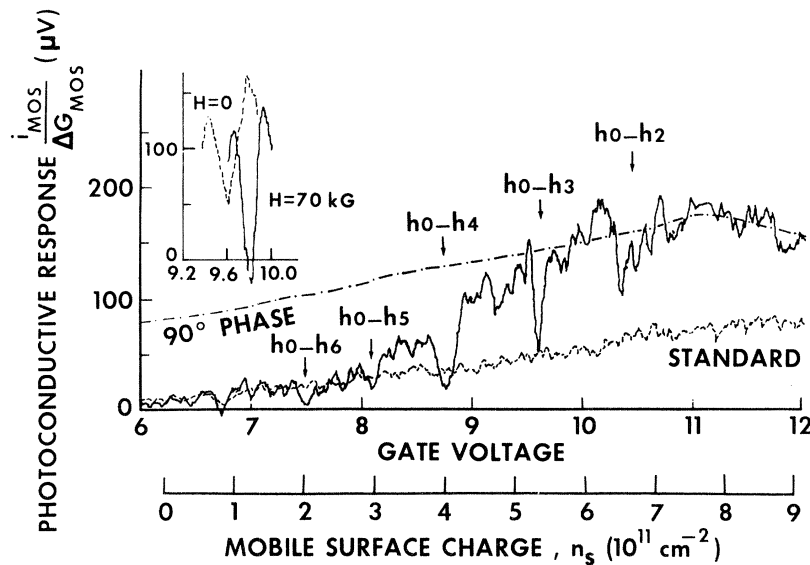


FIG. 2. The photoionization response plotted as a function of both gate voltage and mobile surface electron density (i.e., charge induced above the inversion threshold at 6.2 V). The ordinate, scaled in microvolts, is better defined by the standard response curve which denotes the in-phase signal obtained with the amplitude-modulated double-sideband detection circuit when a photo cell of $\Delta G = 0.1$ mho rms fluctuation was placed electronically in series with the (dark) MOS device. The rising standard response is caused by the sensing current i_{MOS} increasing with inversion; the standard is removed from the circuit prior to irradiation of the MOS device. The reactive component of the interfacial photoconductivity is labeled 90° phase. This component has none of the structure seen on the in-phase response. The dipole transitions from ground heavy subband h_0 to excited heavy subbands h_2 through h_6 are identified by means of the magnetic field accentuation of the $h_0 \rightarrow h_3$ transition photoconductance via the condensation of states near the degeneracy of the h_3 and l_1 subbands. The incident power was about $50 \mu W$.

tion between electric subbands.

Figure 2 shows both the in-phase and out-of-phase photoconductivity response as a function of gate voltage. The in-phase component has imposed on the photoionization background sharp lines corresponding to conductivity *decreases* which we attribute to absorption between electric subbands. The identification of the particular subbands involved in the transitions is facilitated by interpretation of the magnetic field effects. All lines are shifted to higher gate voltage by about 0.2 V in a 70-kG field. As shown in the inset of Fig. 2, associated only with the $h_0 \rightarrow h_3$ is there a strong magnetoresistive increase. For a triangular well defined by any depletion field F , a near degeneracy will occur for the h_3-l_1 and the h_1-l_0 levels because of the masses involved in the two level ladders. In the parallel dispersion only the h_3-l_1 levels cross at small values of k because of the differing curvatures of the h and l bands. We surmise that the decrease in conductivity must reflect decreased mobility in excited states. Those conduction states where band mixing occurs will show further mobility decreases due to the increased conduction-mass component $m = 0.98m_e$ associated with the l states. Applica-

tion of the magnetic field forces a Landau condensation in the density of the states such that in the field all transitions will occur from a single Landau ground state to the first h_3 Landau state which must accentuate the strong band mixing. Thus the magnetoresistance is due to an increased density of states associated with the lower mobility of the mixed h_3-l_1 state, assuming that mobility is inversely proportional to mass.

These interpretations identify the line attributed to the transition $h_0 \rightarrow h_3$ (h_3-l_1 mixed state). Since the relative positions of the other excited states are given by Eq. (2), we may test the labeling further:

$$E_{ci} - E_{c0} = \frac{(ehF)^{2/3}}{(2m_z)^{1/3}} S_i - f(V_i) = h\nu, \quad (4)$$

where $f(V_i)$ is some function of the inverting charge characterizing the position of the ground state. Subtracting for a transition to the j th state, we have

$$\frac{(ehF)^{2/3}}{(2m_z)^{1/3}} (S_i - S_j) = f(V_i) - f(V_j). \quad (5)$$

Figure 3 is a plot of the Airy-function zeros against gate-voltage difference referenced to the

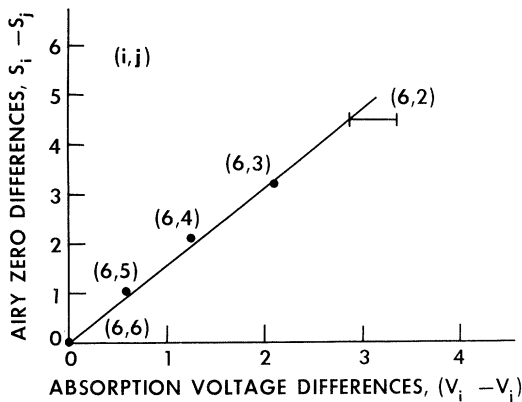


FIG. 3. Plot of the differences of the Airy-function zeros against the measured voltage differences associated with the resistance peaks using the sixth level as reference. The identification is based upon the magnetic field effect associated with the mixed h_3 - l_1 level.

sixth state. With a value of $N_A = 2 \times 10^{14}/\text{cm}^3$ we derive a value of depletion field $F = 8.35 \times 10^3$ V/cm. The data of Fig. 3 then imply that the ground state is depressed nearly linearly with voltage at a rate of 4.5 meV/V or 3.0 meV/(10^{11} electrons/cm 2). Hence, typical line widths are 1–2 meV, a result previously predicted.¹² One may independently determine the rate at which the ground state is depressed by analyzing the voltage shift of the h_0 - h_3 transition in the magnetic field (δV_T can most accurately be determined here since this is the narrowest line). As pointed out by others,² the threshold shift in a magnetic field is due to the zero-point Landau energy $eB/2m$. Taking into account the spin splitting, the ground-state energy becomes $E_{n_0} + eB/2m - g\beta B$. Including valley degeneracy, the state density will be about 1.7×10^{11} electrons/cm 2 for an energy shift of 2.2 meV in 70 kG. Hence the ground state is depressed 2.2 meV by a gate voltage of 0.2 V, giving a rate near threshold of 11 meV/V. This confirms to within a factor of 2 the rate at which the ground state is depressed.

The fact that we do not observe the h_0 - h_1 transition is probably due to the occupation of the h_1

level at the gate voltage necessary to resonate the levels to 44.3 meV.⁴ The structure at the h_0 - h_2 transition may be evidence for the reduction of valley degeneracy in both states.^{1, 2, 11}

In summary, we have demonstrated the existence of voltage-tunable optical transitions between electric subbands at the (001) surfaces of silicon. The band mixing parallel to the surface has allowed identification of the subbands and provided insight into the conductance decrease attributed to occupation of the excited subbands. We believe these measurements to be the first to demonstrate large voltage tunability of electron energy levels in any system.

We would like to acknowledge the help of Stanley Mroczkowski in device fabrication and of Dr. F. A. Stern of the IBM Laboratories in supplying unpublished numerical results.

*Research supported by the U. S. Air Force Office of Scientific Research (AFSC) under Grant No. 68-1506.

¹A. B. Fowler, F. F. Fang, W. E. Howard, and P. J. Stiles, *Phys. Rev. Lett.* **16**, 901 (1966).

²M. Kaplit and J. N. Zemel, *Phys. Rev. Lett.* **21**, 212 (1968).

³C. B. Duke, *Phys. Rev.* **159**, 632 (1967).

⁴F. Stern and W. E. Howard, *Phys. Rev.* **163**, 816 (1967).

⁵D. Colman, R. T. Bate, and J. P. Mize, *J. Appl. Phys.* **39**, 1923 (1968).

⁶A. P. Gnädinger and H. E. Talley, *Solid State Electron.* **13**, 1301 (1970).

⁷A. S. Grove, *Physics and Technology of Semiconductor Devices* (Wiley, New York, 1967).

⁸L. M. Terman, *Solid State Electron.* **5**, 285 (1962).

⁹P. V. Gray and D. M. Brown, *Appl. Phys. Lett.* **8**, 31 (1966).

¹⁰A. Many, Y. Goldstein, and N. B. Grover, *Semiconductor Surfaces* (North-Holland, Amsterdam, 1965), Chap. 6.

¹¹F. F. Fang and W. E. Howard, *Phys. Rev. Lett.* **16**, 797 (1966).

¹²M. E. Alferioff and C. B. Duke, *Phys. Rev.* **168**, 832 (1968).